










Received: 20 December 2020

Revised: 20 April 2021

Accepted: 17 May 2021

NMR-based serum and muscle metabolomics for diagnosis and activity assessment in idiopathic inflammatory myopathies

Anupam Guleria^{1,#}  | Umesh Kumar¹  | Dinesh Kumar¹  | Naveen R^{2,#}  |
Anamika Kumari Anuja²  | Mantabya Kumar Singh⁴  | Pulak Sharma³  |
Vikas Agarwal²  | Ramnath Misra²  | Latika Gupta² 

¹ Centre of Biomedical Research, Sanjay Gandhi Postgraduate Institute of Medical Sciences, Lucknow, India

² Department of Clinical Immunology and Rheumatology, Sanjay Gandhi Postgraduate Institute of Medical Sciences, Lucknow, India

³ Department of Orthopedics, Apex trauma Centre, Sanjay Gandhi Postgraduate Institute of Medical Sciences, Lucknow, India

⁴ Department of Nephrology, Sanjay Gandhi Postgraduate Institute of Medical Sciences, Lucknow, India

Correspondence

Dr. Latika Gupta, Assistant Professor, Department of Clinical Immunology, Sanjay Gandhi Postgraduate Institute of Medical Sciences, Lucknow, India, 226014
Email: drlatikagupta@gmail.com

#These authors contributed equally to this work.

Funding information

Asia Pacific League of Associations for Rheumatology, Grant/Award Number: 2017

Abstract

Objectives: Differentiating smoldering disease activity from weakness due to fatty replacement of atrophied muscle can often be a challenge in the idiopathic inflammatory myositis (IIM). We aimed to identify the metabolic disturbances associated with IIM and if these changes can aid in the assessment of disease activity.

Methods: Metabolic profiles of sera (N = 99) and muscle (N = 21) from patients with IIM (ACR-EULAR criteria) were compared with healthy control (HC) samples (N = 75 for serum and N = 12 for muscle tissues) employing 800 MHz NMR (Nuclear Magnetic Resonance) spectroscopy. Metabolic disparity between IIM and HC was established based on Partial Least Squares Discriminant Analysis (PLS-DA) and the discriminatory metabolites were identified based on variable importance in projection (VIP) statistics (P -value < .05, corrected for false discovery rate (FDR)).

Results: Serum metabolomics profiles were distinctive in IIM as compared to HC, with a visible shift to anaerobic metabolism (increased lactate, low glucose), oxidative defect (high Phenylalanine/tyrosine), decreased muscle mass (low serum creatinine), increased muscle catabolism (increased branched-chain amino acids), and dyslipidemia (higher lipids, higher very low-density lipoprotein [VLDL]/low-density lipoprotein [LDL] ratio, lower polyunsaturated fatty acid [PUFA]). The sera of active IIM patients were characterized by anaerobic metabolism (low glucose), loss of muscle mass (low creatinine, amino acids), and oxidative defect (high Phenylalanine/tyrosine). Three metabolites (isopropanol, succinate, and glycine) were distinctive in muscle tissue metabolomics. NMR-based serum metabolic disparity was lacking between different clinical subsets of IIM.

Conclusion: Serum and muscle tissue metabolomics have the potential to distinguish (a) IIM from HC and (b) active IIM from inactive IIM irrespective of disease subtype.

KEYWORDS

biomarker, metabolomics, muscle, myositis

This is an open access article under the terms of the [Creative Commons Attribution-NonCommercial-NoDerivs License](https://creativecommons.org/licenses/by-nc-nd/4.0/), which permits use and distribution in any medium, provided the original work is properly cited, the use is non-commercial and no modifications or adaptations are made.

© 2021 The Authors. *Analytical Science Advances* published by Wiley-VCH GmbH

1 | INTRODUCTION

The treatment of Idiopathic inflammatory myopathies (IIMs) is challenging, with a majority manifesting with severe muscle disease, and consequent morbidity as well as high early mortality.¹ Up to one-thirds of IIM fail conventional therapy,² the response rates being even lower when the diagnosis and treatment are delayed. Moreover, the IIMs are rare and heterogeneous, with varied presentations, ranging from acute necrotizing IIM,³ to subacute for most, and an indolent course in inclusion body myositis⁴ and certain types of anti-SRP and statin-associated myopathies, leading to limited awareness among primary care providers and patients alike. Thus, the disease incurs significant muscle damage by the time treatment is begun. Partial treatment with low doses of glucocorticoids is common when referral and diagnosis are delayed; and differentiating smoldering disease activity from weakness due to fatty replacement of the atrophied muscle tissues can be an arduous task. Lamentably, conventional biomarkers such as creatine kinase (CK) may be normal in the face of significant muscle wasting, leading to an erroneous diagnosis of inactive disease. With the advent of biologics and better second-line therapies, early identification and timely therapy can prevent permanent muscle atrophy and consequent disability. Unfortunately, there is no marker that can reliably identify the reversible component of inflammation in IIM amid wasted muscle and fibrosis.

Metabolomics, the study of small (<1 kDa) metabolites, is being increasingly used to provide an insight into the ongoing inflammatory, degenerative and neoplastic conditions through the surrogate changes in host metabolism.^{5,6,7,8} Its hypothesis free approach provides the unique opportunity to sample thousands of metabolites derived from carbohydrate, protein, and fat catabolism in an unbiased manner. Nuclear magnetic resonance (NMR)-based metabolic profiling has extensively been carried out over the past several years to study the metabolic alternations in several diseased states including various cancer types, cardiovascular, neurodegenerative, and autoimmune rheumatic diseases.⁹⁻¹⁸ Recently, the NMR-based serum metabolomics studies from our lab have successfully identified active disease in Takayasu's arteritis,^{19,20} and distinguished different phenotypes in ankylosing spondylitis,²¹ suggesting the approach is worth to be explored as surrogate method for improving clinical diagnosis and assessment of disease activity in IIM. Within this framework, the present study was conducted first to identify the distinctive metabolic changes in the sera and tissues of IIM patients, and further to explore its utility to distinguish active from inactive IIM. This was done in a cohort after minimizing environmental deterrents by fasting sampling, rapid transport, adequate storage, and timely processing.^{22,23} Serum and muscle tissues were used for analysis.

2 | MATERIALS AND METHODS

2.1 | Patient and public involvement

Patients with IIM (ACR/EULAR criteria) were enrolled in the MyoCite database with clinical data recorded in a designated case record

KEY MESSAGES

What is already known about this subject?

- Differentiating smoldering disease activity from weakness due to fatty replacement of atrophied muscle can often be a challenge in Idiopathic Inflammatory Myositis (IIM)
- Conventional biomarkers such as creatine kinase (CK) may be normal in the face of significant muscle wasting
- NMR-based metabolomics has successfully identified active disease in Takayasu's arteritis, and distinguished different phenotypes in ankylosing spondylitis.

What does this study add?

- Serum metabolic profiles of IIM patients are distinctively different from HC.
NMR-based serum metabolic profiling has the potential to discriminate active from inactive myositis patients.

How might this impact on clinical practice?

- NMR-based serum metabolic profiling could (i) differentiate active from inactive myositis where conventional markers fail and (ii) aid in critical decisions of whether to continue immune-suppressants or not in the patient.

form and samples (serum and muscle tissue) archived in a biorepository on an institutional ethics cell approved study as previously described.^{22,23,24}

Adults with IIM with Polymyositis (PM), Dermatomyositis (DM), anti-synthetase syndrome (ASSD), and overlap myositis (OM) (myositis in association with another connective tissue disorders (CTD) was as previously described²⁵) were compared with age and gender-matched healthy controls after excluding those with active ongoing infection, myopathies of non-autoimmune origin, pregnancy and menstruation. Those with a myositis disease activity index (MDAAT) of 1 or more with raised muscle enzymes were classified as active disease.²⁶ MDAAT is a validated tool to differentiate active from inactive myositis which employs 10 clinical domains (constitutional symptoms, cutaneous disease activity, skeletal disease activity, gastrointestinal disease activity, pulmonary disease activity, cardiovascular disease activity, other disease activity, extra-muscular global assessment, muscle disease activity, and global disease activity)(26). The presence of MSAs/MAAs (myositis specific antibody/myositis associated antibody) was investigated using the Line immunoassay (G4, Euro-Immune, Lubeck, Germany).

Clinical clusters of PM, DM, OM, and anti-synthetase syndrome (ASSD) were analyzed. Clinical ASSD is defined as presence of myositis by Bohan and Perter criteria plus either ILD or any two of the three features (Arthritis, Raynaud's, Mechanic's hand) not taking into account the antibody profile [anti-RNA synthetase antibodies (ARS)].^{27,28} Clinical ASSD was compared with ARS-based ASSD. Also, metabolites were studied between clinical ASSD, Jo1, and non- Jo1 ARS-based clusters. Metabolites were studied across various MSA and MAA and also

studied between various clinical features. STROBE guidelines were followed for reporting.

2.1.1 | Sample preparation for NMR spectroscopy

The archived serum samples were thawed and homogenized using a vortex mixer for carrying out the NMR experiments. Briefly, the 250 μL of sodium phosphate buffer of strength 50 mM (0.9% saline, prepared in 100% D_2O and pH 7.4) was added to 250 μL of serum to minimize the variation in pH. The obtained mixture was centrifuged at $16,278 \times g$ for 5 min and then 450 μL of this mixture was transferred to 5 mm NMR tubes (Wilmad Glass, USA). A sealed capillary tube holding 1.0 mM TSP (sodium salt of 3-trimethylsilyl-(2,2,3,3-d₄)-propionic acid) dissolved in deuterium oxide (D_2O) was inserted in the NMR tubes as an external reference. Sodium salt of trimethylsilylpropionic acid-d₄ (TSP) and Deuterium oxide (D_2O) were purchased from Sigma-Aldrich (St. Louis, MO, USA).

For muscle metabolomics, one piece of frozen muscle tissue (~20 mg) from muscle biopsy was broken apart in a liquid N_2 -cooled pestle and mortar. Crushed sample was transferred in 2.0 ml MCT containing 1.0 ml phosphate buffer and the resulted mixture was homogenized at -4°C , using ultrasonication. After homogenization, the samples were centrifuged at 4°C ($16,278 \times g$, 5 min) and the 550 μL of supernatant was used for NMR measurements.³⁰

2.1.2 | NMR measurements

The NMR experiments were carried out on Bruker Avance III 800 MHz NMR spectrometer (equipped with a cryoprobe) at 298 K. One-dimensional ^1H NMR spectra were recorded on all serum and muscle samples using the Carr–Purcell–Meiboom–Gill (CPMG) pulse sequence (cpmgrp1d, standard Bruker library pulse program) with pre-saturation of the water signal. The parameters used were as follows: spectral sweep width, 12 ppm; data points, 32768; total relaxation delay (RD), 5 s; number of transients, 128; and T_2 filtering (for suppressing the broad signals of large macromolecules including proteins) was obtained with an echo time of 200 μs repeated 300 times, resulting in a total duration of effective echo time of 60 ms. All the spectra were then processed using Topspin-2.1 (Bruker NMR data Processing Software) using a standard Fourier transformation (FT) procedure following manual phase and baseline correction. Prior to FT, each FID was zero-filled to 65536 data points and multiplied by a 0.3 Hz exponential line-broadening function. To aid the spectral assignment, 2D homonuclear (^1H - ^1H TOCSY) and heteronuclear (^1H - ^{13}C HSQC) NMR experiments were also recorded on selected samples with the details as reported previously.³¹ The spectral resonances in the ^1H CPMG NMR spectra were assigned using the 800 MHz compound spectral database library of the Chenomx NMR suite with pH set at 7.2 for all the samples (Chenomx Inc., Edmonton, AB, Canada) along with the help of ^1H - ^1H TOCSY and ^1H - ^{13}C HSQC NMR spectra and further validated using

publically available databases (such as HMDB: <http://www.hmdb.ca/> and BMRB: www.bmr.b.wisc.edu/metabolomics) and previously reported NMR assignments of metabolites in literature.^{30–35} A confidence level ranging from 1 to 5 was assigned to each metabolite as described elsewhere.³⁵

2.1.3 | Multivariate statistical analysis

Prior to the multivariate statistical data analysis, all the NMR spectra were referenced internally to methyl peak of lactate (at $\delta = 1.31$ ppm) followed by the spectral binning using AMIX package (Version 3.9.15, Bruker) in the chemical shift range δ (0.5–8.5 ppm). The chemical shift region δ 4.7–5.2 ppm was excluded to eliminate the residual signal of water and distorted region due to imperfect water suppression. The serum NMR spectra were binned into 0.02 ppm integrated spectral buckets and each spectral bin was further normalized using the total spectral intensity to eliminate the dilution effect among samples. The resulting binned data matrix was then exported to Microsoft office excel, included with class information for samples and converted into text file containing data in CSV (i.e., comma-separated values) format and used for multivariate data analysis through various analysis modules of MetaboAnalyst 4.0 (an open-access web-based metabolomics data processing tool).^{36,37} Pareto scaling was applied for binned serum data matrix during the processing steps prior to the multivariate analysis. Principal component analysis (PCA) was performed for initial overview of the grouping trend within the data set and outlier detection. Next, the supervised Partial Least Squares Discriminant Analysis (PLS-DA) was carried out to reveal group separations between the groups and to identify the discriminatory metabolites responsible for group separation. To avoid the over-fitting of the PLS-DA model, 10-fold cross-validation algorithm was used. For muscle metabolic profiling, the NMR spectra obtained on the muscle tissue were analyzed using PROFILER-Module of CHENOMX, and concentrations of selected metabolites were estimated in all the 21 muscle samples of IIM patients and 12 muscle samples. The resulted quantitative muscle metabolic profiles of IIM and HC groups were then compared using the PCA and PLS-DA analysis. The PLS-DA models were cross-validated by a permutation analysis (100 times), and the resulting goodness-of-fit parameter R^2 and the goodness of prediction parameter Q^2 were used to assess the quality of the PLS-DA models. The metabolites responsible for the discrimination in the PLS-DA model were identified from the VIP (variable importance on projection) score with value > 1.0 . The obtained variables are further evaluated for statistical significance using *t*-test for two group analyses and ANOVA for multiple group comparisons. A 0.05 level of significance, that is, *P*-value $< .05$ was used as the standard for statistical significance. The additional *P*-values adjustment for multiple testing was carried out using the Benjamini-Hochberg false discovery rate (FDR) correction method.³⁸ Further, the specificity and selectivity of the obtained potential marker metabolites were checked using receiver operating characteristic (ROC) curves analysis. The quantitative estimation of the significant metabolites was done with the help of Chenomx NMR Suite v8.1.

TABLE 1 List of discriminatory metabolites responsible for separation between IIM and HC groups. The metabolic biomarkers were identified using PLS-DA analysis with VIP score > 1.0 as the cut-off value for the discrimination significance and P -value ≤ 0.05 for statistical significance (the up and down arrows represent, increased (\uparrow) and decreased (\downarrow) levels in IIM patients compared to healthy controls). The corresponding area under the ROC curve is also enlisted

Characteristics	Serum IIM (n = 99)	Serum HC (n = 75)	Muscle HC (n = 12)
Age (years, median, IQR)	36 (30–42)	28 (23–32)	29.5 (24.5–41.7)
Gender-female (F:M)	78:21	62:13	3:09
Disease duration (months/IQR)	6 (3–12.5)	–	–
<i>Diagnosis</i>			Muscle from
DM	43 (43.4)		Lower limb: 9
ASS	21 (21.2)		(femur # 7, ACL/PCL repair knee 2)
OM	22 (22.2)		Upper limb:3
PM	11 (11.1)		(Olecranon # 3)
CAM	2 ²		
Active: Inactive	44:55:00		

Abbreviation: IIM-Idiopathic inflammatory myopathies, IQR-Interquartile range DM-Dermatomyositis, ASS -anti-synthetase syndrome, OM-overlap myositis, PM-polymyositis, CAM-Cancer associated myositis, ILD-Interstitial lung disease, ACL-Anterior cruciate ligament, PCL-Posterior cruciate ligament, # stands for Fracture.

The data that support the findings of this study has been uploaded on ZENODO (<https://zenodo.org/record/4661033>) (39) and is available without undue reservation for further studies on request to the corresponding author.

3 | RESULTS

3.1 | Patient characteristics

Sera [n = 99, 36^{30–42} years, M/F 1:3.7 (21:78)], and muscle [n = 21, 48^{39–55} years, M/F 1.1:1 (11:10)] from patients classifiable as myositis by the ACR-EULAR criteria were compared with healthy controls (HC)[Serum HC: n = 75, 27^{23–32} years, M/F 1:4.35 (14:61), Muscle HC: n = 12, 29.5 (24.5–41.7) years, M/F 3:1 (9:3)] (Table 1). Of the 99, 44 had active myositis (defined by MDAAT > 1). Of the 21 IIM muscle biopsies, none were from inactive IIM due to ethical concerns of obtaining biopsy in inactive group. All the 21 muscle biopsies had evidence of myositis in histopathology and had raised muscle enzymes.

3.2 | Multivariate statistical analysis to access the metabolic variations between HC and IIM groups

Figure 1 depicts the representative 1D ¹H CPMG NMR spectra of serum samples obtained from a healthy control and IIM with identified signals from lipid and membrane metabolites, amino acids, energy metabolites along with some other metabolites like acetate, acetone, acetoacetate, and so on. The spectral resonances in the NMR spectra were assigned with the help of 2D ¹H-¹³C HSQC spectra as shown in Figure S1 with metabolites annotation. Table S1 enlists the metabolite assignments of major spectral resonances detected in ¹H NMR spectra

of serum samples with their confidence levels. Multivariate analysis was carried out on ¹H NMR spectra recorded on IIM and HC sera with the aim to extract the IIM-induced changes in the serum metabolic profiles. The initial overview of the data by PCA analysis did not reveal any significant difference between IIM and HC groups (Figure S2). Therefore, PLS-DA analysis was carried out to investigate the metabolic differences between the two groups. As shown in Figure 2A, the PLS-DA score plots revealed a clear separation, with high values of R^2 and Q^2 parameters ($R^2 = 0.89$ and $Q^2 = 0.81$) demonstrating a satisfactory fit of model with good predictive power without overfitting of the original model. The robustness of the derived PLS-DA model was further evaluated using a random permutation test with 100 permutations and the corresponding cross-validation plot shown in Figure S3A revealed that both the permuted R^2 and Q^2 values on the left were lower than the corresponding original points on the right with significant positive slopes. Also, the negative intercept (intercepts: $R^2 = (0.0, 0.233)$; $Q^2 = (0.0, -0.221)$) of the Q^2 regression line indicates the statistical significance of PLS-DA model and rules out the random or overfitting of the data. Figure S3B illustrates the loading plot of metabolites between HC and IIM patients corresponding to PLS-DA score plot shown in Figure 2A. The upward and downward peaks in the loading plot correspond to the elevated and depleted metabolites in the sera of IIM patients, respectively. Figure 2B illustrates the VIP scores plot of metabolites responsible for the separation between HC and IIM patients in PLS-DA score plot shown in Figure 2A. Among the statistically significant variables identified using VIP values (VIP > 1.0) in the PLS-DA model and the t-test (FDR corrected $P < .05$), a panel of 29 discriminatory metabolites were identified exhibiting statistically significant difference between the groups as tabulated in Table 2.

We found that compared to healthy controls, a number of metabolites showed increased concentration in serum of IIM patients, such as amino acids, 3-Hydroxybutyrate, lipids (including fatty acids), NAG

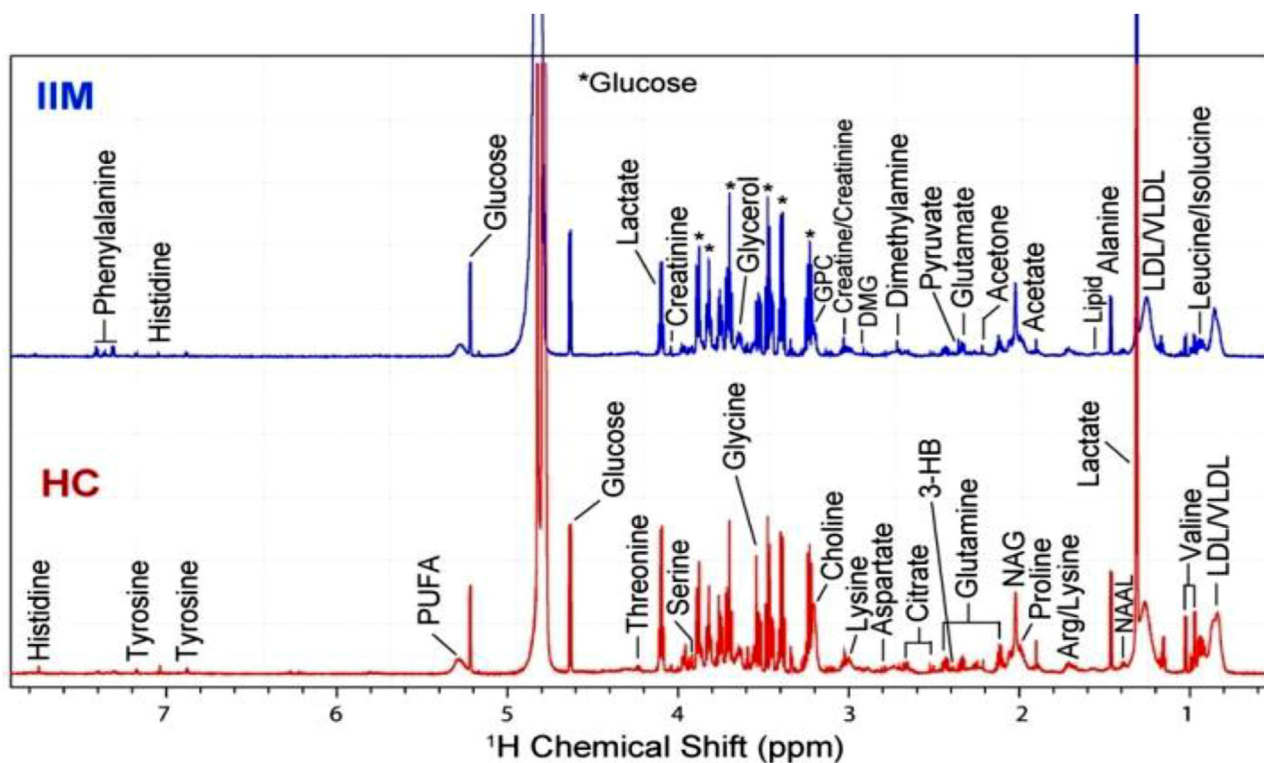


FIGURE 1 Stack plot of representative ^1H CPMG NMR spectra of serum samples obtained from an IIM patient and a healthy control along with the assignment of serum metabolites as annotated in the figure. The abbreviations used are: 3-HB: 3-Hydroxybutyrate; Arg: Arginine; DMG: Dimethylglycine; GPC: Glycerophosphocholine; LDL/VLDL: Low/very-low density lipoproteins; NAAL: Na-acetyl-L-Lysine; NAG: N-acetylglucoproteins; PUFA: polyunsaturated fatty acids

(N-acetyl glycoproteins), pyruvate, creatine, glucose, glycerol, acetoacetate, dimethylamine, and Na-acetyl lysine, while serum levels of several others metabolites such as lactate, LDL, VLDL, alanine, choline, glycerophosphocholine, and PUFA were found to be decreased in the IIM patients (Figure 2C). The obtained area under the Receiver's operating characteristic (AUROC) values are enlisted in Table 2 with only 19 metabolites exhibiting AUC greater than 0.75. The metabolites (AUROC > 0.90) 3-Hydroxybutyrate, arginine, pyruvate, acetoacetate, and dimethylamine have the highest potential of being the serum biomarkers for IIM patients. All these metabolites were significantly up-regulated in IIM patients as compared to the HC.

3.3 | Multivariate statistical analysis to access the metabolic variations in clinical clusters of IIM

Further, the serum metabolic profiles were compared between the clinical subtypes and the results are summarized below:

A. The initial overview of the data by PCA analysis did not reveal any sample clustering and group separation and neither the PLS-DA models showed any discrimination between clinical subtypes of IIM (i.e., PM, DM, and OM; Figure S4A) suggesting these subtypes have poor serum metabolic disparity. The R^2 and Q^2 values were negative or unsatisfactory for the models and t -test were not significant.

- B. Similarly, the patients with clinical diagnosis of ILD, arthritis, bulbar weakness, amyopathic presentation, and skin rashes (Gottron's, heliotrope, mechanic's hands, cutaneous ulcers and photosensitivity,) showed no serum metabolic disparity compared to those without these clinical diagnoses (Figure S4B-E).
- C. IIM with a clinical ASSD without ARS was similar to ARS group (Figure S4F). Clinical ASSD, Jo1, and non- Jo1 ASSD were similar in clusters (Figure S5). The initial overview of the data by PCA analysis did not reveal any significant difference and neither in PLS-DA. The R^2 and Q^2 values were negative or unsatisfactory for the models and t -test were not significant.
- D. IIM clusters defined by distinct MSAs also exhibited significant overlap (Figure S6A-E). The presence and absence of MAA (Figure S6F) and antinuclear antibody (ANA) (Figure S6B) were not discriminative in the PLS-DA score plots. The initial overview of the data by PCA analysis did not reveal any significant difference and neither in PLS-DA. The R^2 and Q^2 values were negative or unsatisfactory for the models and t -test were not significant.

3.4 | Metabolic profiling of active and inactive IIM

PLS-DA analysis was carried out to compare the metabolic profiles of inactive and active IIM patients. We found that the metabolic profiling of patients with active and inactive disease exhibited a clear

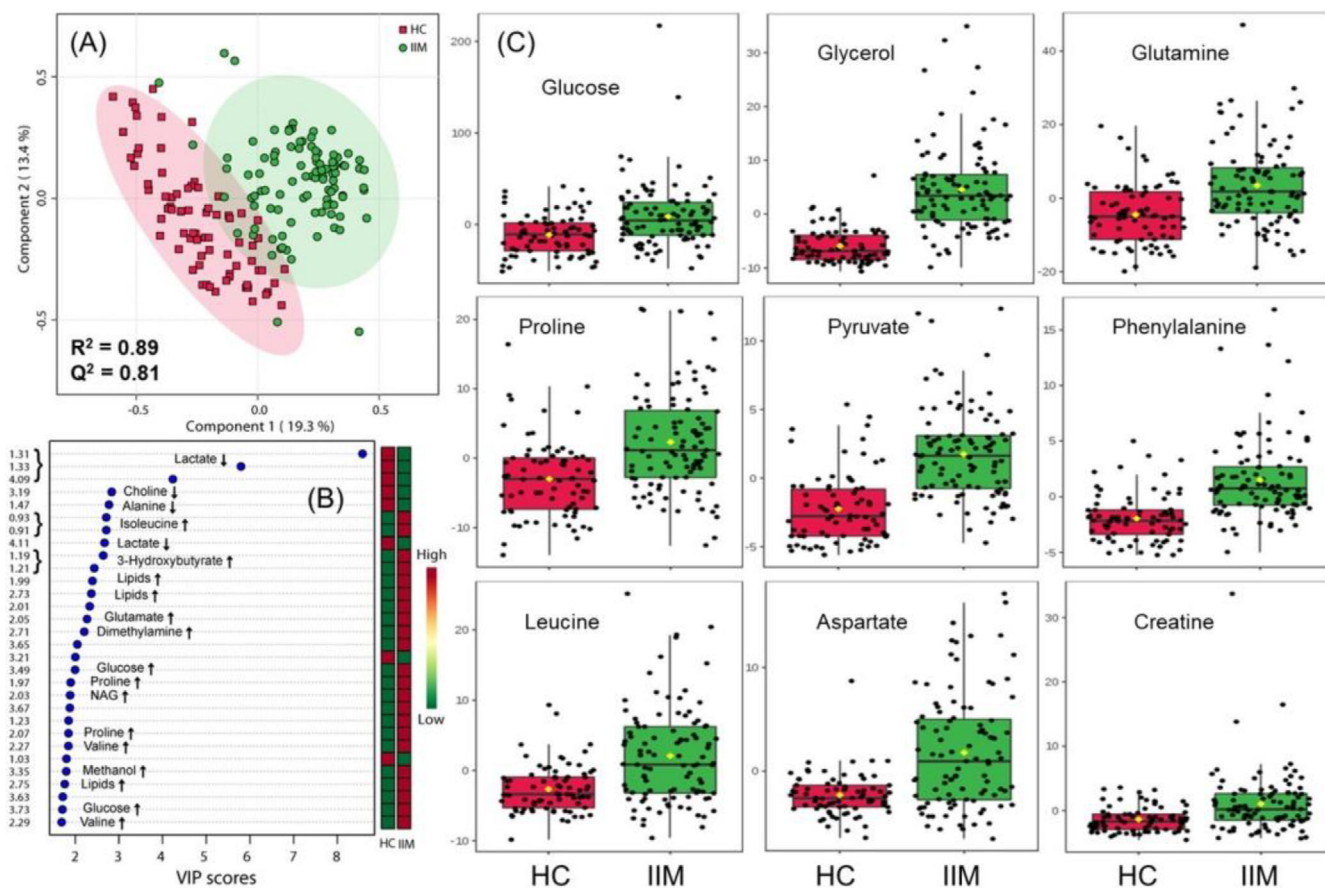


FIGURE 2 (A) The 2D PLS-DA score plot derived from analysis of CPMG ^1H NMR spectra of serum samples showing discrimination between IIM and HC groups. The colored ovals represent the 95% confidence intervals for each group. (B) The VIP score plot used to identify the metabolite entities responsible for the discrimination of IIM and HC in PLS-DA score plot shown in (A). The color bar in the VIP score plot represent whether the corresponding metabolite levels are high or low, where red represents increase and green represents decrease in the levels. (C) Representative box-cum-whisker plots showing quantitative variations of concentration for maker serum metabolites. For presented metabolite entities, the VIP score > 1 and statistical significance is at the level of $P \leq .05$ after FDR correction. In the box plots, the boxes denote interquartile ranges, horizontal line inside the box denote the median, and bottom and top boundaries of boxes are 25th and 75th percentiles, respectively. Lower and upper whiskers are 5th and 95th percentiles, respectively

clustering of the two groups (within the group) but with very mild discrimination as shown in the PLS-DA score plot Figure 3A (as also evident from R^2 and Q^2 values less than 0.6 along with the cross-validation plot shown in Figure S3C). VIP score plot is shown in Figure 3B depicting the discriminatory metabolites and representative box plots of the serum metabolic concentrations are shown in Figure 3D. The list of discriminatory metabolites responsible for separation between active and inactive IIM patients and exhibiting the statistically significant difference between the two groups are tabulated in Table 3 along with their AUROC values. Compared to inactive IIM patients, sera of active IIM patients had low levels of amino acids (such as glutamine, valine, alanine, histidine, leucine, proline, and aspartate), suggesting a loss of muscle mass. Glycerol, choline, creatinine, and glucose were low as well. Lactate and glutamate levels were also low in active IIM patients as compared to inactive IIM patients. High Phenylalanine/tyrosine in active myositis was seen as indicative of oxidative defects (Figure S7).

3.5 | Muscle tissue metabolic profiling of HC and IIM patients

PLS-DA analysis was carried out to compare the metabolic profiling of muscle tissue obtained from HC and IIM patients. We found that the muscle tissue metabolic profiling of IIM patients exhibited a clear clustering and discrimination from HC as shown in the PLS-DA score plot Figure 4A. The permutation plot for the derived PLS-DA model showing R^2 and Q^2 values is shown in Figure S3D indicating the validity of the original model. The corresponding cross-validation parameters plot is shown Figure 4B and the VIP scores, AUROC are enlisted in Table S2. We found that the three discriminatory metabolites (isopropanol, succinate, and glycine) were responsible for the separation of two groups. The levels of glucose, creatine, lactate, taurine, and glycerol were also found to be decreased in IIM group as compared to HC. Figure 4C depicts the ROC curve and the relative concentrations of few of these metabolites as a box cum whisker plots.

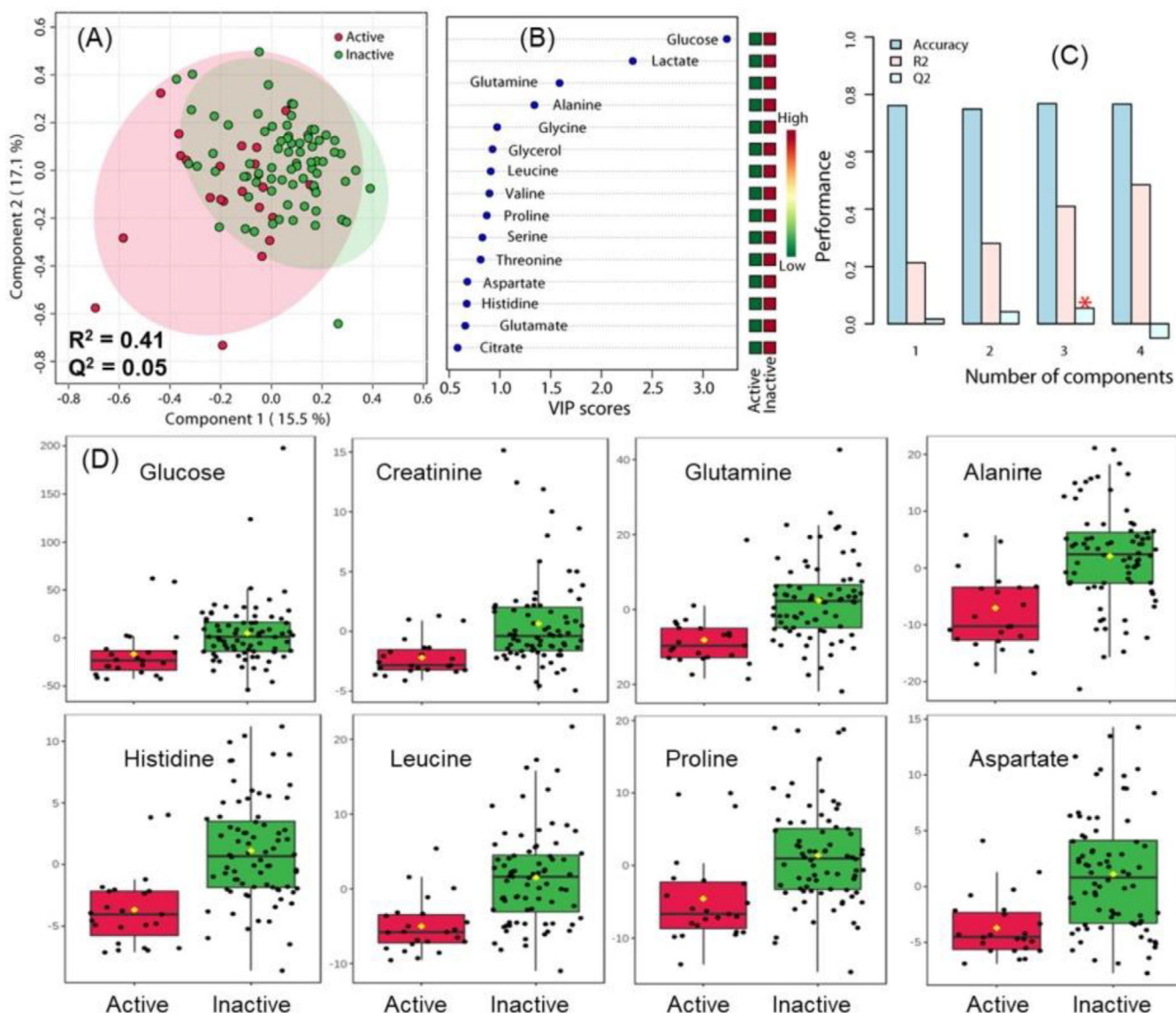


FIGURE 3 PLS-DA model between active and inactive IIM patients: (A), (B), and (C) represent 2D score plot, VIP score plots, and cross-validation parameters, respectively. VIP score plot shown has been derived for PLS-DA components highlighted by red asterisk (*) and depicting metabolite entities contributing in the group separation. The green and red boxes on the right side of each VIP score plot indicate the low and high serum levels of corresponding metabolites in each group under investigation. (D) Representative box-cum-whisker plots showing quantitative variations of the concentrations of serum metabolites for active and inactive IIM patients. For presented metabolite entities, statistical significance is at the level of $P \leq .05$ after FDR correction. In the box plots, the boxes denote interquartile ranges, horizontal line inside the box denote the median, and bottom and top boundaries of boxes are 25th and 75th percentiles, respectively. Lower and upper whiskers are 5th and 95th percentiles, respectively

4 | DISCUSSION

We found that the serum and muscle metabolomics is distinctive in IIM, with the potential to discriminate active from inactive disease. The changes identified in the serum are largely indicative of a shift to anaerobic metabolism, shrinking muscle mass, and accentuated oxidative stress, potentially a reflection of altered metabolome in the inflamed muscles. Further, serum metabolomics was similar across the clinical and serological clusters of IIM. Thus, metabolomics could be distinct markers of disease activity uninfluenced by the heterogeneity of IIM.

4.1 | Anaerobic switch in metabolism

In spite of the well-established inflammatory origins of IIM, the non-immune mechanisms of muscle dysfunction have received much attention lately. Muscle weakness precedes the appearance of inflammatory infiltrates on muscle biopsy specimens in H+T+ mice with MHC-1 conditional upregulation,⁴⁰ and is attributable to deregulated cellular bioenergetics arising from dysfunction of Adenosine monophosphate (AMP) deaminase-1 early in the inflamed muscles.⁴¹ MR spectroscopy imaging of the muscle has further

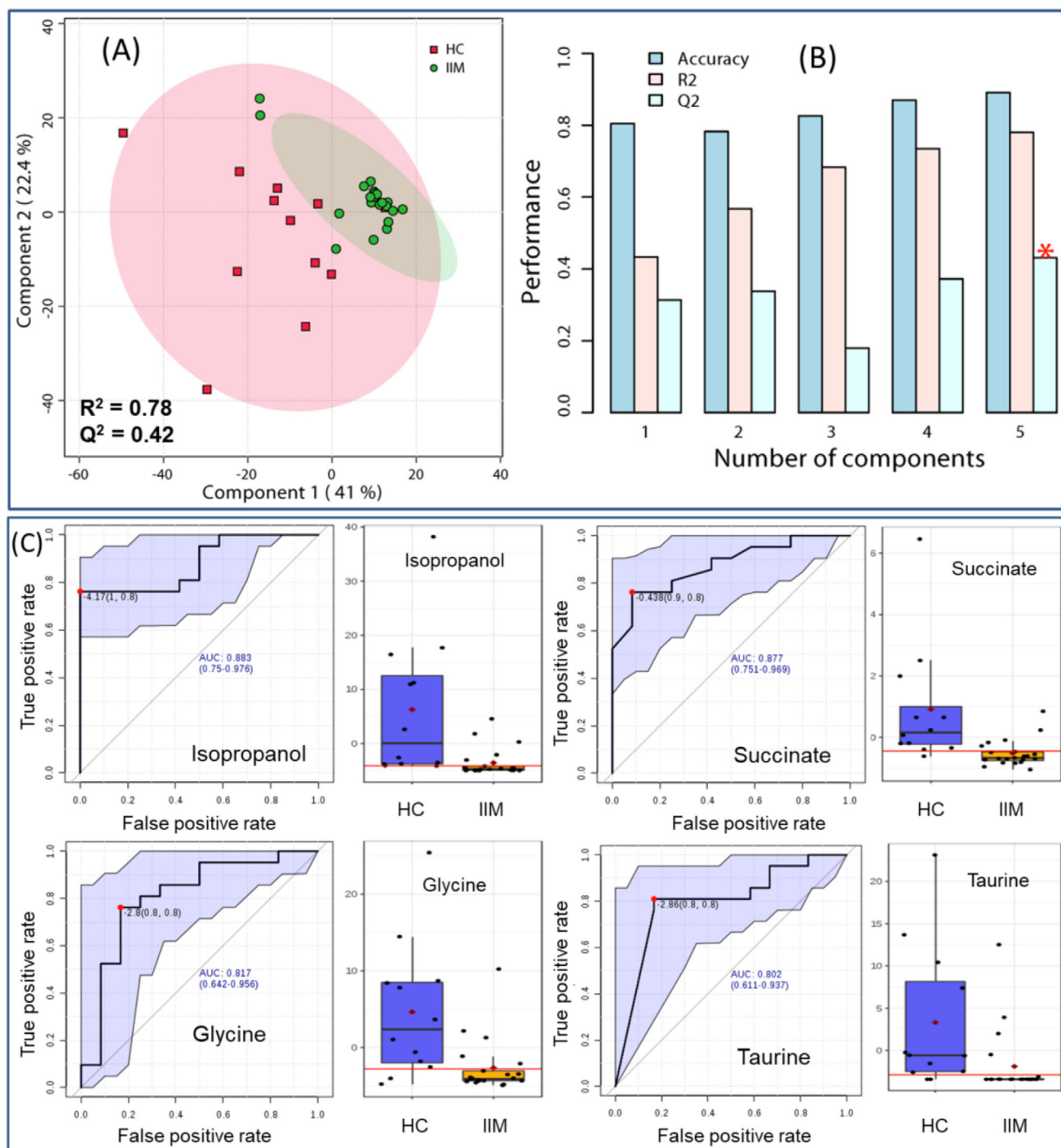


FIGURE 4 (A) PLS-DA score plot derived from the analysis of ^1H CPMG NMR spectra of muscle tissue from IIM and HC along with the corresponding cross-validation parameters shown in (B). (C) Area under the receiver operating characteristic curve (AUROC) calculated for selected differential biomarkers in HC and IIM patients. ROC curve and representative box-cum-whisker plots showing the quantitative variation of the concentrations of discriminatory metabolites for IIM and HC. For isopropanol, succinate, and glycine, statistical significance is at the level of $P \leq .05$ after FDR correction; while for taurine, statistical significance is at the level of $P \leq .05$. In the box plots, the boxes denote interquartile ranges, horizontal line inside the box denote the median, and bottom and top boundaries of boxes are 25th and 75th percentiles, respectively. Lower and upper whiskers are 5th and 95th percentiles, respectively

TABLE 2 List of discriminatory metabolites responsible for separation between IIM and HC groups. The metabolic biomarkers were identified using PLS-DA analysis with VIP score > 1.0 as the cut-off value for the discrimination significance and P-value ≤ .05 for statistical significance (the up and down arrows represent, increased (↑) and decreased (↓) levels in IIM patients compared to healthy controls). The corresponding area under the ROC curve is also enlisted

#	Metabolite	¹ H shift (ppm)	IIM vs HC	AUROC
1	LDL/VLDL	0.87	↓	0.590034
2	BCAA-Isoleucine	0.93	↑	0.786667
3	BCAA-Leucine	0.95	↑	0.663569
4	3-Hydroxybutyrate	1.19	↑	0.942896
5	Lactate	1.33	↓	0.835152
6	Alanine	1.47	↓	0.752323
7	Arginine	1.65	↑	0.914613
8	Proline	1.97	↑	0.833805
9	Lipids	1.99	↑	0.742088
10	N-Acetyl Glycoprotein	2.03	↑	0.669899
11	Glutamate	2.05	↑	0.766599
12	Proline	2.07	↑	0.822896
13	Acetone	2.23	↑	0.828013
14	Lipids	2.25	↑	0.791246
15	Acetoacetate	2.27	↑	0.93037
16	Pyruvate	2.37	↑	0.954747
17	Glutamine	2.45	↑	0.660067
18	Aspartate	2.65	↑	0.896835
19	Dimethylamine	2.73	↑	0.974815
20	Lipids	2.75	↑	0.8633
21	Na-Acetyl Lysine	2.97	↑	0.84532
22	Creatine	3.02	↑	0.716768
23	Choline	3.19	↓	0.823165
24	Glycerophosphocholine	3.21	↓	0.659731
25	Glucose	3.48	↑	0.690148
26	Glycine	3.55	↑	0.673131
27	Glycerol	3.65	↑	0.818182
28	Polyunsaturated Fatty acids	5.29	↓	0.67569
29	Phenylalanine	7.31	↑	0.830644
30	Phenylalanine/Tyrosine ratio		↑	0.816607

affirmed decreased concentrations of Adenosine diphosphate, AMP, and phosphocreatine in DM.⁴² Besides, these changes can be identified as low creatinine and inorganic phosphate using NMR spectroscopy in the muscles, even in clinically amyopathic cases before subsequent progression to full-blown disease.⁴² Anaerobic metabolism was characterized in the current study by an increased lactate production and low glucose. This may explain the high fatigability and inability to perform repetitive tasks in day-to-day activities.⁴³ Besides, elevated Phenylalanine/tyrosine in serum of active as compared with inactive IIM indicate

TABLE 3 List of discriminatory metabolites responsible for separation between active and inactive IIM patients along with the corresponding VIP score, P-values (unadjusted and adjusted for multiple comparisons (FDR)), and AUROC

#	Metabolite	VIP Score	P value	P value (FDR)	AUROC
1	Glucose	3.215	.006253	.0086348	0.768878719
2	Lactate	2.1644	.042076	.045192	0.705377574
3	Glutamine	1.5593	3.38E-05	.00019603	0.827803204
4	Alanine	1.3576	1.86E-05	.00015849	0.792620137
5	Glycine	0.9888	.001227	.001872	0.732837529
6	Glycerol	0.98114	.000529	.0011707	0.782036613
7	Leucine	0.9658	9.44E-06	.0001369	0.830091533
8	Valine	0.93934	2.19E-05	.00015849	0.813501144
9	Proline	0.87938	.000356	.00093954	0.77402746
10	Serine	0.85858	.000319	.00093954	0.760869565
11	Threonine	0.83575	.000228	.0008248	0.767162471
12	Aspartate	0.71296	5.11E-05	.00024674	0.794622426
13	Histidine	0.70747	1.88E-06	5.45E-05	0.839816934
14	Glutamate	0.6862	.0236	.027376	0.708524027
15	Citrate	0.59032	.000327	.00093954	0.783180778
16	Methionine	0.50833	.00108	.0017401	0.805491991
17	Choline	0.49957	.000208	.0008248	0.778604119
18	Isoleucine	0.49147	.000677	.0013091	0.807208238
19	Creatinine	0.41851	.000792	.001351	0.798340961

an oxidation defect and catabolic state.^{44,45} Previous literature in Takayasu arteritis also recorded high serum glutamate levels in active disease with Indian Takayasu arteritis activity score (ITAS-A) > 4.¹⁹

4.2 | Decreased muscle mass

Serum creatinine is a rough estimate of muscle mass. Creatine produced by liver is broken to creatinine by muscle which is excreted in urine.⁴⁶ The only previous study on metabolomics in IIM was in children with Juvenile dermatomyositis (JDM), where urinary creatinine/choline ratio correlated with damage.⁴⁷ We found low serum creatinine in active as compared with inactive IIM. While a low muscle mass in damage is known and expected (and is part of damage indices), the use of fall in creatinine concentration as an early event to identify activity has not been previously described. Serum creatinine concentrations by nephelometry are crude and lack sensitivity, hence conjunction of NMR with nephelometry could add value to creatinine measurements for determining activity.⁴⁸ This tool merits further exploration in data sets of IIM with stratified disease activity, damage, and an objective measurement of muscle mass. Besides, the observation of low branch chain amino acids (BCAA, obtained by breakdown of muscle protein) in the serum in active IIM further substantiates loss of muscle proteins.⁴⁹

4.3 | Lipid metabolism

Lipid metabolism is altered in myositis. There were higher lipid levels and lower PUFA levels in myositis when compared to HC. This could pave way for increased cardiovascular risks in myositis patients.⁵⁰ Similarly, in SLE, there is a clear differential pattern of lipids characterized by high lipids and low PUFA levels.⁵¹

4.4 | IIM versus healthy

An elevation in BCAA and NAG in IIM patients as compared to HC signifies an inflammatory state, which is expected given their role in oxidative stress, macrophage metabolism, and cytokine production (interleukin-1,2, TNF alpha, and interferon production).⁴⁹ The fall in creatinine values is a surrogate for a declining muscle mass in the event of the disease.

4.5 | Muscle metabolomics

NMR has shown considerable promise in metabolomics analysis of tissue samples.^{52,53} As the metabolic changes in serum could be the reflection of metabolic changes in muscles, therefore we found similar alterations in the muscle tissue of active IIM as in serum, that is, low glucose, creatinine, and BCAA. Our comparisons of metabolic events in the muscle in active and inactive IIM were limited by the absence of a biopsy in inactive disease due to ethical issues. *In vivo* imaging of the muscle may further enhance understanding of the events in the future.

Overall, the results presented in this paper revealed distinguished metabolic signatures of IIM patients as compared to HC. Further, NMR-based metabolic profiling may be able to differentiate active disease from damage in myositis patients. Another study by using Liquid chromatography-mass spectrometry (LCMS), showed a distinctive signature in bronchoalveolar lavage fluids in patients with overlap myositis and DM/PM.⁵⁴ Most other biomarkers are limited by the heterogeneity of IIM, while we found no difference in metabolomics profiles in the various subsets, which lends it a unique advantage over other conventional markers when assessing activity. Standard muscle biomarkers like CK can be low in patients with muscle wasting, including body myositis, myositis associated with neoplasia, and early presentations of polymyositis and dermatomyositis.⁵⁵ CK levels do not necessarily correlate with disease activity and with a cut-off of 500 they have moderate sensitivity and specificity (66% and 77%, respectively).⁵⁶ CK levels cannot differentiate between IIM subtypes and other causes like metabolic/genetic muscle diseases. This is true for other muscle enzymes which are the standard biomarkers of myositis. Further muscle enzyme levels are influenced by gender, exercise intensity, duration, and muscle mass.⁵⁵ Serum and muscle metabolomics may help in those situations where conventional biomarkers fail.

The validation of the obtained results on larger prospective cohorts will be required in future longitudinal studies. It is important to mention here that we haven't compared with MRI of muscle for disease

activity that is the limitation of the study. Further, the current study was performed with a limited number of active and inactive IIM samples, and thus the observed metabolic changes should further be validated on larger patient groups. Another limitation is the heterogeneity among the selected patients' population (lifestyle, gender, diet, environmental factors, etc.) and the lack of inclusion of quality controls (such as pool of all the analyzed samples) in the study.

5 | CONCLUSION

In conclusion, serum and muscle metabolomics are distinctive in IIM. Metabolites in the serum such as low creatinine and branch chain amino acids suggestive of a shrinking muscle mass, low glucose and high lactate from an anaerobic metabolism and higher phenylalanine/tyrosine ratio from oxidation defects may distinguish active from inactive myositis.

AUTHOR CONTRIBUTIONS

LG, AA, and MK collected and analyzed the clinical data while AG, DK, NR, and UK were involved in metabolomics analysis. All authors were involved in writing and reviewing the manuscript for critical intellectual inputs.

ACKNOWLEDGMENTS

A.G. acknowledges the Science and Engineering Research Board, Govt. of India for SERB Women Excellence Award (SB/WEA-08/2019) and DST (Department of Science and Technology) for INSPIRE Faculty Award (LSBM-120).

ETHICS APPROVAL

Institute Ethics Committee of the Sanjay Gandhi Postgraduate Institute of Medical Sciences. EIC number 2017-41-IP-76

CONFLICT OF INTEREST

The authors declared no conflict of interest.

DATA AVAILABILITY STATEMENT

The data that support the findings of this study has been uploaded on ZENODO (<https://zenodo.org/record/4661033>) and is available without undue reservation for further studies on request to the corresponding author.

ORCID

Anupam Guleria  <https://orcid.org/0000-0002-4158-2241>

Umesh Kumar  <https://orcid.org/0000-0002-0961-8048>

Dinesh Kumar  <https://orcid.org/0000-0001-8079-6739>

Naveen R  <https://orcid.org/0000-0003-2014-3925>

Anamika Kumari Anuja  <https://orcid.org/0000-0003-0722-8756>

Mantabya Kumar Singh  <https://orcid.org/0000-0003-2747-2182>

Pulak Sharma  <https://orcid.org/0000-0002-7270-8177>

Vikas Agarwal  <https://orcid.org/0000-0002-4508-1233>

Ramnath Misra  <https://orcid.org/0000-0001-7921-4199>

Latika Gupta  <https://orcid.org/0000-0003-2753-2990>

REFERENCES

- Muhammed H, Gupta L, Zanwar AA, et al. Infections are leading cause of in-hospital mortality in indian patients with inflammatory myopathy. *J Clin Rheumatol*. 2021;27(3):114-119.
- Lilleker J, Murphy S, Cooper R. Selected aspects of the current management of myositis. *Ther Adv Musculoskelet Dis*. 2016;8(4):136-144.
- Pinal-Fernandez I, Casal-Dominguez M, Mammen AL. Immune-Mediated Necrotizing Myopathy. *Curr Rheumatol Rep*. 2018;20(4):21.
- Dimachkie M, Barohn R. Inclusion Body Myositis. *Semin Neurol*. 2012;32(03):237-245.
- Carrola J, Rocha CM, Barros AS, et al. Metabolic Signatures of Lung Cancer in Biofluids: nMR-Based Metabonomics of Urine. *J Proteome Res*. 2011;10(1):221-230.
- Guma M, Tiziani S, Firestein GS. Metabolomics in rheumatic diseases: desperately seeking biomarkers. *Nat Rev Rheumatol*. 2016;12(5):269-281.
- Armitage EG, Barbas C. Metabolomics in cancer biomarker discovery: current trends and future perspectives. *J Pharm Biomed Anal*. 2014;87:1-11.
- Fitzpatrick M, Young SP. Metabolomics – A novel window into inflammatory disease. *Swiss Med Wkly*. 2013;143:w13743.
- Spratlin JL, Serkova NJ, Eckhardt SG. Clinical applications of metabolomics in oncology: a review. *Clin Cancer Res Off J Am Assoc Cancer Res*. 2009;15(2):431-440.
- Griffin JL, Atherton H, Shockcor J, Atzori L. Metabolomics as a tool for cardiac research. *Nat Rev Cardiol*. 2011 Sep 20;8(11):630-643.
- Slupsky CM, Steed H, Wells TH, et al. Urine metabolite analysis offers potential early diagnosis of ovarian and breast cancers. *Clin Cancer Res Off J Am Assoc Cancer Res*. 2010;16(23):5835-5841.
- Serkova NJ, Glunde K. Metabolomics of cancer. *Methods Mol Biol*. 2009;520:273-295.
- Serum metabolic profiling in inflammatory bowel disease - PubMed [Internet]. [cited 2021 Feb 14]. Available from: <https://pubmed.ncbi.nlm.nih.gov/22488632/>
- Warde N. Osteoarthritis: identification of a metabolomic biomarker for knee OA. *Nat Rev Rheumatol*. 2010;6(7):381.
- Weljie AM, Dowlatabadi R, Miller BJ, Vogel HJ, Jirik FR. An Inflammatory Arthritis-Associated Metabolite Biomarker Pattern Revealed by 1H NMR Spectroscopy. *J Proteome Res*. 2007;6(9):3456-3464.
- Scriver R, Casadei L, Valerio M, Priori R, Valesini G, Manetti C. Metabolomics approach in allergic and rheumatic diseases. *Curr Allergy Asthma Rep*. 2014;14(6):445.
- van Wietmarschen HA, Dai W, van der Kooij AJ, et al. Characterization of rheumatoid arthritis subtypes using symptom profiles, clinical chemistry and metabolomics measurements. *PLoS ONE*. 2012;7(9):e44331.
- Kumar U, Kumar A, Singh S, et al. An elaborative NMR based plasma metabolomics study revealed metabolic derangements in patients with mild cognitive impairment: a study on north Indian population. *Metab Brain Dis*. 2021;36(5):957-968.
- Jain A, Kumar D, Guleria A, et al. NMR-Based Serum Metabolomics of Patients with Takayasu Arteritis: relationship with Disease Activity. *J Proteome Res*. 2018 Sep 7;17(9):3317-3324.
- Kumar U, Jain A, Guleria A, et al. Circulatory Glutamine/Glucose ratio for evaluating disease activity in Takayasu arteritis: a NMR based serum metabolomics study. *J Pharm Biomed Anal*. 2020;180:113080.
- Wang W, Yang G, Zhang J, et al. Plasma, urine and ligament tissue metabolite profiling reveals potential biomarkers of ankylosing spondylitis using NMR-based metabolic profiles. *Arthritis Res Ther*. 2016;18(1):244.
- Naveen R, Anuja AK, Rai MK, Agarwal V, Gupta L. Development of the MyoCite biobank: cost-efficient model of public sector investigator-driven biobank for idiopathic inflammatory myositis. *Indian J Rheumatol*. 2020;15(6):194.
- Gupta L, Appani S, Janardana R, et al. Meeting report: myoIN – Pan-India collaborative network for myositis research. *Indian J Rheumatol*. 2019;14(2):136.
- Mehta P, Gupta L. Combined Case Record Forms for collaborative datasets of patients and controls of idiopathic inflammatory myopathies. *Indian J Rheumatol Myositis*. 2020. Accept Publ. https://www.researchgate.net/publication/343125493_Combined_case_record_forms_for_collaborative_datasets_of_patients_and_controls_of_idiopathic_inflammatory_myopathies.
- Nuño-Nuño L, Joven BE, Carreira PE, et al. Overlap myositis, a distinct entity beyond primary inflammatory myositis: a retrospective analysis of a large cohort from the REMICAM registry. *Int J Rheum Dis*. 2019;22(8):1393-1401.
- Rider LG, Werth VP, Huber AM, et al. Measures of adult and juvenile dermatomyositis, polymyositis, and inclusion body myositis: physician and Patient/Parent Global Activity, Manual Muscle Testing (MMT), Health Assessment Questionnaire (HAQ)/Childhood Health Assessment Questionnaire (C-HAQ), Childhood Myositis Assessment Scale (CMAS), Myositis Disease Activity Assessment Tool (MDAAT), Disease Activity Score (DAS), Short Form 36 (SF-36), Child Health Questionnaire (CHQ), physician global damage, Myositis Damage Index (MDI), Quantitative Muscle Testing (QMT), Myositis Functional Index-2 (FI-2), Myositis Activities Profile (MAP), Inclusion Body Myositis Functional Rating Scale (IBMFRS), Cutaneous Dermatomyositis Disease Area and Severity Index (CDASI), Cutaneous Assessment Tool (CAT), Dermatomyositis Skin Severity Index (DSSI), Skindex, and Dermatology Life Quality Index (DLQI). *Arthritis Care Res*. 2011;63(Suppl 1):S118-157.
- Bohan A, Peter JB. Polymyositis and Dermatomyositis. *N Engl J Med*. 1975;292(7):344-347.
- Solomon J, Swigris JJ, Brown KK. Myositis-related interstitial lung disease and antisynthetase syndrome. *J Bras Pneumol Publicacao Of Soc Bras Pneumol E Tisilogia*. 2011;37(1):100-109.
- Kumar D, Pandey G, Bansal D, et al. NMR-based urinary profiling of lactulose/mannitol ratio used to assess the altered intestinal permeability in acute on chronic liver failure (ACLF) patients. *Magn Reson Chem*. 2017;55(4):289-296.
- Beckonert O, Keun HC, Ebbels TMD, et al. Metabolic profiling, metabolomic and metabonomic procedures for NMR spectroscopy of urine, plasma, serum and tissue extracts. *Nat Protoc*. 2007;2(11):2692-2703.
- Guleria A, Misra DP, Rawat A, et al. NMR-Based Serum Metabolomics Discriminates Takayasu Arteritis from Healthy Individuals: a Proof-of-Principle Study. *J Proteome Res*. 2015;14(8):3372-3381.
- Wishart DS, Jewison T, Guo AC, et al. HMDB 3.0—The Human Metabolome Database in 2013. *Nucleic Acids Res*. 2013;41(Database issue):D801-7.
- Guleria A, Bajpai NK, Rawat A, Khetrpal CL, Prasad N, Kumar D. Metabolite characterisation in peritoneal dialysis effluent using high-resolution ¹H and ¹H-¹³C NMR spectroscopy: characterisation of PD effluent metabolites. *Magn Reson Chem*. 2014;52(9):475-479.
- Guleria A, Pratap A, Dubey D, et al. NMR based serum metabolomics reveals a distinctive signature in patients with Lupus Nephritis. *Sci Rep [Internet]*. 2016;6(1). <https://doi.org/10.1038/srep35309>.
- Walejko J, Chelliah A, Keller-Wood M, Gregg A, Edison A. Global Metabolomics of the Placenta Reveals Distinct Metabolic Profiles between Maternal and Fetal Placental Tissues Following Delivery in Non-Labored Women. *Metabolites*. 2018;8(1):10.
- Xia J, Wishart DS. Using MetaboAnalyst 3.0 for Comprehensive Metabolomics Data Analysis. *Curr Protoc Bioinforma*. 2016;55(1):14.10.1-14.10.91.
- Xia J, Psychogios N, Young N, Wishart DS. MetaboAnalyst: a web server for metabolomic data analysis and interpretation. *Nucleic Acids Res*. 2009;37(Web Server):W652-60.

38. Hochberg Y, Benjamini Y. More powerful procedures for multiple significance testing. *Stat Med.* 1990;9(7):811-818.
39. Kumar D, Guleria A, Kumar U, R N, Gupta L. NMR based Serum and Muscle Metabolomics for Diagnosis and Activity Assessment in Idiopathic Inflammatory Myopathies [Internet]. *Zenodo.* 2021. <https://zenodo.org/record/4661033>. [cited 2021 Apr 20]. Available from.
40. Nagaraju K, Raben N, Loeffler L, et al. Conditional up-regulation of MHC class I in skeletal muscle leads to self-sustaining autoimmune myositis and myositis-specific autoantibodies. *Proc Natl Acad Sci U S A.* 2000;97(16):9209-9214.
41. Coley W, Rayavarapu S, Pandey GS, et al. The molecular basis of skeletal muscle weakness in a mouse model of inflammatory myopathy. *Arthritis Rheum.* 2012;64(11):3750-3759.
42. Park JH, Olsen NJ, Jr LK, et al. Use of magnetic resonance imaging and p-31 magnetic resonance spectroscopy to detect and quantify muscle dysfunction in the amyopathic and myopathic variants of dermatomyositis. *Arthritis Rheum.* 1995;38(1):68-77.
43. Bertolucci F, Neri R, Dalise S, Venturi M, Rossi B, Chisari C. Abnormal lactate levels in patients with polymyositis and dermatomyositis: the benefits of a specific rehabilitative program. *Eur J Phys Rehabil Med.* 2014;50(2):9.
44. Wannemacher RW Jr, Klainer AS, Dinterman RE, Beisel WR. The significance and mechanism of an increased serum phenylalanine-tyrosine ratio during infection. *Am J Clin Nutr.* 1976;29(9):997-1006.
45. Richards DA, Tolia CM, Sgouros S, Bowery NG. Extracellular glutamine to glutamate ratio may predict outcome in the injured brain: a clinical microdialysis study in children. *Pharmacol Res.* 2003;48(1):101-109.
46. Brosnan JT, Brosnan ME. Creatine metabolism and the urea cycle. *Mol Genet Metab.* 2010;100:S49-52.
47. Chung Y-I, Rider LG, Bell JD, et al. Muscle metabolites, detected in urine by proton spectroscopy, correlate with disease damage in juvenile idiopathic inflammatory myopathies. *Arthritis Care Res.* 2005;53(4):565-570.
48. Cassiède M, Nair S, Dueck M, et al. Assessment of 1H NMR-based metabolomics analysis for normalization of urinary metals against creatinine. *Clin Chim Acta Int J Clin Chem.* 2017;464:37-43.
49. The effect of BCAA supplementation upon the immune response. *Medicine & Science in Sports & Exercise [Internet].* 2020. Available from: <https://journals.lww.com/acsm-msse/pages/articleviewer.aspx?year=2000&issue=07000&article=00005&type=Fulltext>
50. Coyle K, Rother KI, Weise M, Ahmed A, Miller FW, Rider LG. Metabolic Abnormalities and Cardiovascular Risk Factors in Children with Myositis. *J Pediatr.* 2009;155(6):882-887.
51. Ouyang X, Dai Y, Wen J, Wang L. 1H NMR-based metabolomic study of metabolic profiling for systemic lupus erythematosus. *Lupus.* 2011;20(13):1411-1420.
52. Emwas A-H, Roy R, McKay RT, et al. Recommendations and Standardization of Biomarker Quantification Using NMR-Based Metabolomics with Particular Focus on Urinary Analysis. *J Proteome Res.* 2016;15(2):360-373.
53. Gupta L, Majumder S, Aggarwal A, Misra R, Lawrence A. Serum Fatty Acid-Binding Protein 3 Levels Differentiate Active from. *Indian J Rheumatol.* 2020(15):187-190.
54. Passadore I, Iadarola P, Di Poto C, et al. 2-DE and LC-MS/MS for a Comparative Proteomic Analysis of BALf from Subjects with Different Subsets of Inflammatory Myopathies. *J Proteome Res.* 2009;8(5):2331-2340.
55. Benveniste O, Goebel H-H, Stenzel W. Biomarkers in Inflammatory Myopathies—An Expanded Definition. *Front Neurol [Internet].* 2019;10. <https://www.ncbi.nlm.nih.gov/pmc/articles/PMC6558048/>. [cited 2020 Dec 19]. Available from.
56. Cardy CM, Potter T. The predictive value of creatine kinase, EMG and MRI in diagnosing muscle disease. *Rheumatology.* 2007;46(10):1617-1618.

SUPPORTING INFORMATION

Additional supporting information may be found online in the Supporting Information section at the end of the article.

How to cite this article: Guleria A, Kumar U, Kumar D, et al. NMR-based serum and muscle metabolomics for diagnosis and activity assessment in idiopathic inflammatory myopathies. *Anal Sci Adv.* 2021;2:515–526. <https://doi.org/10.1002/ansa.202000171>